ЖУРНАЛ СТРУКТУРНОЙ ХИМИИ

2015. Том 56, № 8 *Декабрь* *С. 1532 – 1536*

UDC 541.49:546.14:541.6

THE MOLECULAR DESIGNS AND PROPERTIES OF ASYMMETRIC HETEROCYCLES $(HBrBN_3)_n$ (n = 1—4)

Q.Y. Xia[1,2], D.X. Ma[2], D.J. Li[2], B.H. Li[2], X.Q. Wang[2], G.F. Ji[1]

[1]*National Key Laboratory of Shock Wave and Detonation Physics, Institute of Fluid Physics, Chinese Academy of Engineering Physics, Mianyang, P. R. China*
E-mail: xiaqiying@163.com, cyfjkf@caep.ac.cn
[2]*School of Chemistry and Chemical Engineering, Linyi University, Linyi, P. R. China*

Received May, 06, 2014

The structures and properties of asymmetric heterocycles $(HBrBN_3)_n$ (n = 1—4) are systematically studied at the B3LYP/6-31G* level. The molecules $(HBrBN_3)_n$ (n = 2—4) have the core structures of a 2n-membered ring with alternating boron and α-nitrogen atoms. The relationships between geometrical parameters and oligomerization degree n are discussed. The calculated IR spectra have four main characteristic regions. Trends in thermodynamic properties with temperature and oligomerization degree n are discussed. Thermodynamic analysis of the gas-phase oligomerizations shows that formation of the most stable heterocycles $(HBrBN_3)_n$ (n = 2—4) is enthalpy driven in the range of 200—800 K.

DOI: 10.15372/JSC20150803

K e y w o r d s: asymmetric clusters $(HBrBN_3)_n$ (n = 1—4), density functional theory (DFT), structures, IR spectra, stabilities.

INTRODUCTION

The extensive studies on boron azides are motivated by the fact that these molecules have been shown to be good precursors for boron nitride (BN) film deposition [1]. The inorganic and organic boron azide compounds including $(CH_3)_2BN_3$, $(n\text{-}C_3H_7)_2BN_3\cdot Py$, $(C_6H_5)_2BN_3\cdot Py$, $(n\text{-}C_4H_9)_2BN_3$, $(BX_2N_3)_3$ (X = F, Cl, Br), $[(C_6F_5)_2BN_3]_2$ and $[(C_6F_5)_2BN_3]_3$ etc. have been synthesized and studied experimentally [2—5]. However, experimental structure data are very limited, and most of these compounds have to be studied by theoretical methods. The structures of monomeric BCl_2N_3 and $(CH_3)_2BN_3$ have been studied by using *ab initio* calculation, and estimation of thermodynamic stability of BX_2N_3 with respect to the dimerization and trimerization reactions have been gained [6—10].

Obviously, boron azides reported above are all symmetric heterocycles. For Al and Ga, such low-temperature single source precursors, $(RR'MN_3)_n$ (M = Al, Ga; R = CH_3, H; R′ = Cl, Br; n = 3—4), have been synthesized and investigated in vapor deposition (CVD) studies [11—13]. Here, motivated by and based on previously studies on asymmetric cyclic gallane azides and aluminum azide, we performed density functional theory (DFT) investigations on the asymmetric molecules $(HBrBN_3)_n$ (n = 1—4). The results shed some light into the emergence of their bulklike behavior with the increase in the size of the clusters.

COMPUTATIONAL METHODS

In order to find out the lowest-energy structures of $(HBrBN_3)_n$ (n = 1—4), we designed possible models of the initial structures. The $(HBrBN_3)_n$ (n = 1—4) were optimized using DFT at the B3LYP/6-

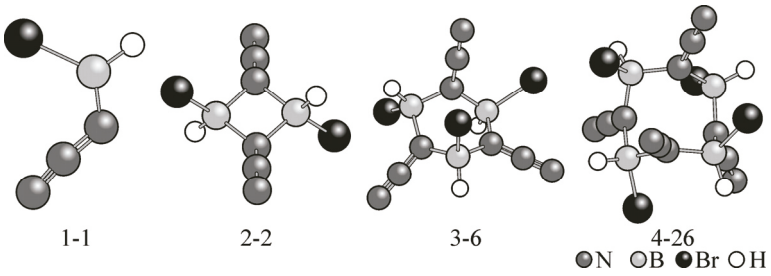

Fig. 1. Lowest-energy structures for $(HBrBN_3)_n$ (n = 1—4)

31G* level [14, 15]. Moreover, electronic structures, vibrational properties and thermodynamic properties were analyzed for the most stable isomers. Since the DFT calculated harmonic vibrational frequencies are usually larger than those observed experimentally, they are scaled by a factor of 0.96 [16].

Computations were performed with the Gaussian 03 package [17]. The optimizations were performed without any symmetry restrictions using the default convergence criteria in the programs. All optimized structures were characterized to be true local energy minima on the potential energy surfaces without imaginary frequencies.

RESULTS AND DISCUSSIONS

Optimized geometries and energies. Fig. 1 shows the lowest-energy structure for each member of the $(HBrBN_3)_n$ family (n = 1—4). Table 1 lists the most stable geometrical parameters, energies and symmetries. When n = 1, two stably planar structures (1-1 and 1-2) were obtained. They have the same symmetry, but different bond lengths. When n = 2—4, four dimers (2-1, 2-2, 2-3, and 2-4), eleven trimers (3-1 ~ 3-11) and fifty three tetramers (4-1 ~ 4-53) are obtained, all of which are cyclic. They do not have B—B and N_α—N_α bonds. Judged by the total energies, the most stable isomers are 1-1, 2-2, 3-6 and 4-26. There are some minor changes in binding energies of $(HBrBN_3)_n$ for each n value, but the average binding energies are hardly affected by isomerism.

As is seen from Table 1, the N_α—N_β bonds are longer than N_β—N_γ. This can be interpreted as a higher bond order for the terminal N—N bond, showing a pre-formation of the N_2 molecule. Moreover, we also find that the oligomerization degree n has an important influences on the geometries. With the oligomerization degree n increasing, the average value of the N_β—N_γ bond lengths decreases, while the average values of the N_α—N_β, B—H and B—Br bond lengths increase. The N_α—B distances in the trimers and tetramers are shorter compared to those in the dimers. This may be attributed to the increase in the strain in the four-membered ring. The increasing N_α—N_β, B—H and B—Br bond lengths imply that it could be easy to eliminate N_2 (N_β—N_γ), H_2 and Br^- groups to yield BN material. For the monomer (n = 1), azide group is slightly bent with N_α—N_β—N_γ angles of 172.6°. In the oligomers $(HBrBN_3)_n$ (n = 2—4), azide groups are nearly linear with N_α—N_β—N_γ angles in the range of 176.8—179.6°. The bond angles N_α—B—N_α and B—N_α—B increase as the cycle becomes larger, while N_β—N_α—B bond angles decrease. The B—N_α—B bond angles are consistently larger than N_α—B—N_α bond angles, with the difference increasing with the size of the cycle growthing.

T a b l e 1

Ranges of the bond lengths (Å), *bond angles* (deg.), *energies* ($kJ \cdot mol^{-1}$) *and symmeties of asymmetric clusters* $(HBrBN_3)_n$ (n = 1—4) *optimized at the* DFT-B3LYP *level*

Parameter	1-1	2-2	3-6	4-26
N_β—N_γ	1.133	1.130	1.125—1.130	1.126
N_α—N_β	1.242	1.243	1.249—1.259	1.258
B—N_α	1.422	1.605—1.607	1.575—1.619	1.576—1.609
B—H	1.184	1.191	1.190—1.193	1.191
B—Br	1.922	1.981	1.991—2.018	2.010
N_α—N_β—N_γ	172.6	176.9	176.8—179.4	179.5—179.6
N_β—N_α—B	123.7	125.0—126.1	116.5—119.5	114.7—117.4
B—N_α—B		94.1	121.9—124.1	127.1
N_α—B—N_α		85.9	101.3—103.6	105.2
E	–7250106.54	–14500227.41	–21750427.76	–29000592.39
ZPE	71.68	150.24	231.39	311.05
Symmetry	C_s	C_i	C_1	C_2

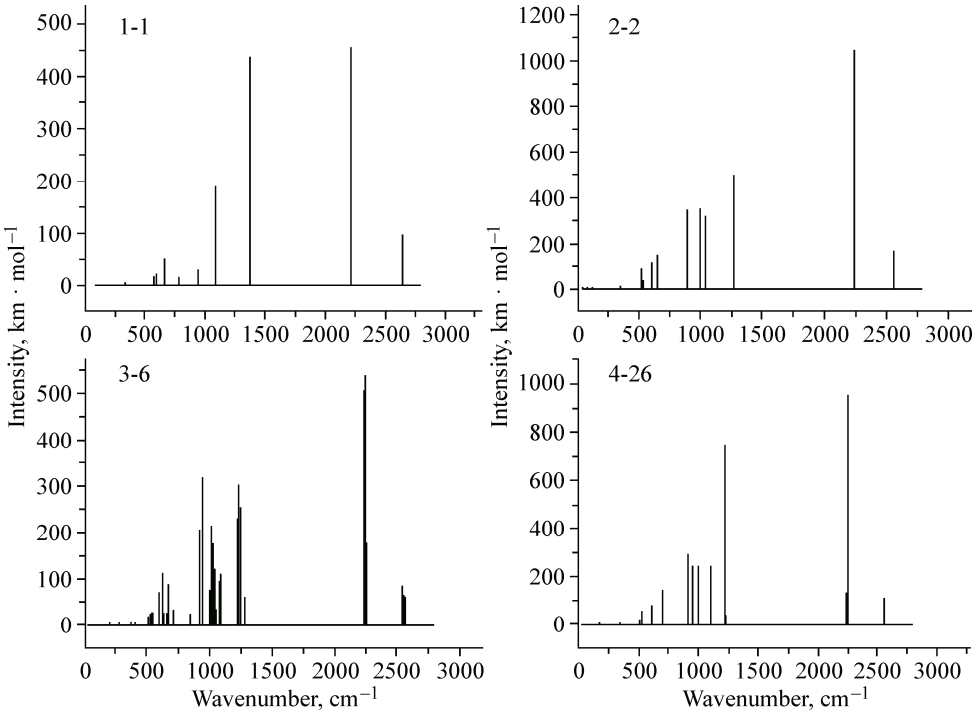

Fig. 2. IR spectra of the most stable structures of $(HBrBN_3)_n$ (n = 1—4)

IR spectrum. The simulated IR spectra of the most stable isomers of $(HBrBN_3)_n$ (n = 1—4) based on the scaled harmonic vibrational frequencies are investigated at the DFT-B3LYP level. As is well known, IR spectra are basic characteristics of compounds and are fingerprints for identification of substances. Moreover, IR spectra have a direct relation with the thermodynamic properties. However, to the best of our knowledge, there are no experimental IR data for the title compounds. Therefore, it is of great significance to calculate IR spectra for both theoretical and practical reasons. From Fig. 2, it can be seen that there are four main characteristic regions associated with the N_3 asymmetric and symmetric stretching, B—H stretching, and the fingerprint region.

The stretching vibration of B—H appears above 2500 cm^{-1}, and the number of frequencies equals to the number of B—H bonds, e.g. dimer $(HBrBN_3)_2$ with two B—H bonds has two vibrational bands at 2560 cm^{-1} and 2562 cm^{-1} correspondingly. The modes at 2216 ~ 2251 cm^{-1} with the strongest absorption intensities are associated with the characteristic N_3 asymmetric stretching vibrations, and in this region, the number of vibration equals to that of azido groups. For example, 3A has three bands at 2231 cm^{-1}, 2240 cm^{-1}, and 2250 cm^{-1}. The characteristic N_3 symmetric stretching modes are located in the frequency range of 1218 ~ 1367 cm^{-1} with strong intensities. In this region, the number of vibration also equals to that of azido groups. For example, 4B has four bands at 1218 cm^{-1}, 1226 cm^{-1}, 1226 cm^{-1}, and 1247 cm^{-1}. The weak peak at less than 1100 cm^{-1} is the fingerprint region, which is composed of stretching of rings, the stretching of B—Br, the wagging and scissoring of H—B—Br, and the N_3 deformation vibrations. This can be used to identify isomers. Meanwhile, the oligomerization degree n have an effect on the vibrational frequencies and intensities. The N_3 asymmetric stretching moves to higher frequency (hypsochromic phenomenon) as the cluster becomes larger, however, the N_3 symmetric stretching moves to lower frequency (bathochromic phenomenon).

Thermodynamic properties. According to the calculated IR, the thermodynamic properties ($C^0_{p,m}$, S^0_m, and H^0_m) of the most isomers of $(HBrBN_3)_n$ (n = 1—4) ranging from 200 K to 800 K were evaluated and presented in Table 2. With the increase in temperature, the calculated thermodynamic functions monotonically increase. This is because the vibrational movement is intensified at the higher temperature and makes more contributions to the thermodynamic functions, while at lower temperatures the main contributions to the thermodynamic functions come from the translations and rotations of the molecules. Taking 1-A as an example, the temperature-dependent relationships for $C^0_{p,m}$, S^0_m,

Table 2

Thermodynamic properties for the most stable isomers of $(HBrBN_3)_n$ (n = 1—4) *for each size at different temperature*[a]

Compound	T	200	298.2	300	400	500	600	700	800
1-1	$C^0_{p,m}$	61.17	74.98	75.21	86.11	94.28	100.56	105.53	109.54
	S^0_m	291.40	318.48	318.94	342.14	362.28	380.04	395.93	410.29
	H^0_m	9.22	15.93	16.07	24.16	33.2	42.95	53.27	64.03
2-2	$C^0_{p,m}$	126.30	159.55	160.09	184.95	202.94	216.43	226.91	235.27
	S^0_m	401.74	458.65	459.64	509.29	552.59	590.84	625.02	655.88
	H^0_m	16.92	31.02	31.31	48.63	68.07	89.07	111.26	134.38
3-6	$C^0_{p,m}$	191.94	242.57	243.40	281.54	309.42	330.38	346.65	359.60
	S^0_m	503.23	589.74	591.24	666.78	732.75	791.10	843.30	890.46
	H^0_m	24.72	46.15	46.60	72.95	102.57	134.61	168.49	203.83
4-26	$C^0_{p,m}$	260.09	328.16	329.27	380.39	417.73	445.77	467.53	484.83
	S^0_m	569.02	686.17	688.2	790.32	879.42	958.17	1028.58	1092.18
	H^0_m	32.13	61.15	61.76	97.37	137.37	180.61	226.32	273.97

[a] Units: T, K; $C^0_{p,m}$, J·mol^{-1}·K^{-1}; S^0_m, J·mol^{-1} ·K^{-1}; H^0_m, kJ·mol^{-1}.

and H^0_m in the range of 200—800 K. can be expressed as shown in Fig. 3, *a*. It is obvious that, as the temperature increases, the gradients of $C^0_{p,m}$ and S^0_m decrease, while that of H^0_m increases constantly. However, since the coeffcients of T^2 are very small, these correlations approximate linear equations.

In addition, the oligomerization degree n-dependent relations for $C^0_{p,m}$, S^0_m, and H^0_m of the most stable isomers of $(HBrBN_3)_n$ (n = 1—4) at 298.2 K can be expressed in Fig. 3, *b*. With the increase of the oligomerization degree n, all the thermodynamic functions increase. One could find that, $C^0_{p,m}$, S^0_m, and H^0_m increase on an average by 84 J·mol^{-1}·K^{-1}, 123 J·mol^{-1}·K^{-1}, and 15 kJ·mol^{-1}, respectively, when one more $HBrBN_3$ is added.

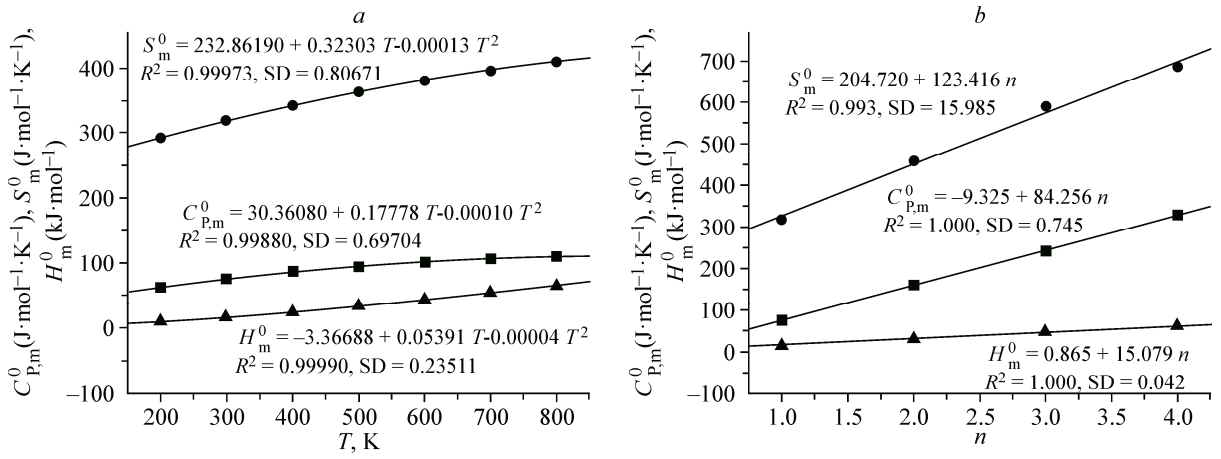

Fig. 3. The correlations between the thermodynamic functions ($C^0_{p,m}$, S^0_m, and H^0_m) and the temperature (T) (*a*) or the oligomerization degree n (*b*)

Table 3

Oligomerization enthalpies and Gibbs free energies at different temperature [a]

Processes	T	200	298.2	300	400	500	600	700	800
1-1 → 2-2	ΔH	–9.25	–8.57	–8.56	–7.42	–6.06	–4.56	–3.01	–1.41
	ΔG	26.96	44.60	44.91	62.57	79.92	96.98	113.77	130.35
1-1 → 3-6	ΔH	–95.40	–94.10	–94.07	–91.99	–89.49	–86.70	–83.78	–80.72
	ΔG	–21.20	14.95	15.61	51.87	87.56	122.71	157.36	191.61
1-1 → 4-26	ΔH	–147.64	–145.46	–145.41	–142.16	–138.32	–134.08	–129.65	–125.04
	ΔG	–28.32	29.81	30.86	89.14	146.53	203.12	258.95	314.15

[a] Units: T, K, ΔH, kJ·mol^{-1}, ΔG, kJ·mol^{-1}.

Based on the calculated thermodynamic functions, the theoretical enthalpies (ΔH) and Gibbs free energies (ΔG) of various oligomerizations in the $HBrBN_3 + HBrBN_3$ system in the range of 200—800 K are compiled in Table 3. The oligomerization enthalpies are negative in the range of 200—800 K, which reveals that the oligomerizations are thermodynamically favorable. The values of ΔG are positive at 298.2 K, which indicates the oligomerization can not occur spontaneously.

CONCLUSIONS

The structural feature, energies, IR spectra, and thermodynamic properties of asymmetric molecules $(HBrBN_3)_n$ (n = 1—4) have been calculated at the DFT-B3LYP level. All the structures (n = 2, 3, 4) are cyclic with alternating B and N_α atoms. The bond lengths outside of the rings increase as the cycle is enlarged, which show that it could easily eliminate N_2 (N_β—N_γ), H_2 and Br^- groups to yield BN material. The calculated IR spectra have four main characteristic regions: B—H stretching, the N_3 asymmetric stretching, the N_3 symmetric stretching, and the most complicated fingerprint region. Thermodynamic properties are linearly correlated with the oligomerization degree n as well as the temperature. The calculated thermodynamic properties show that all the oligomerizations are enthalpy driven at 298.2 K, however, all the oligomerizations can not occur spontaneously.

We gratefully thank the National Natural Science Foundation of China (No. 21203086), Shandong Provincial Natural Science Foundation (No. ZR2012BL09), Shandong Provincial Key Laboratory of Water and Soil Conservation and Environmental Protection (No. STKF201009), and the National Key Laboratory Fund for Shock Wave and Detonation Physics Research of the China Academy of Engineering Physics (No. 9140C671101110C6709).

REFERENCES

1. *Mulinax R.L., Okin G.S., Coombe R.D.* // J. Phys. Chem. – 1995. – **99**. – P. 6294.
2. *Paetzold P.I., Hansen H.J.* // Z. Anorg. Allg. Chem. – 1966. – **345**. – P. 79.
3. *Wiberg N., Joo W.C., Schmid K.H.* // Z. Anorg. Allg. Chem. – 1972. – **394**. – P. 197.
4. *Fraenk W., Klapötke T.M., Krumm B. et al.* // Chem. Commun. – 2000. – P. 667.
5. *Fraenk W., Klapötke T.M., Krumm B. et al.* // J. Chem. Soc., Dalton Trans. – 2000. – P. 4635.
6. *Johnson L.A., Sturgis S.A., Al-Jihad I.A. et al.* // J. Phys. Chem. A. – 1999. – **103**. – P. 686.
7. *Hausser-Wallis R., Oberhammer H., Einholz W. et al.* // Inorg. Chem. – 1990. – **29**. – P. 3286.
8. *Fraenk W., Klapötke T.M.* // J. Fluorine Chem. – 2001. – **111**. – P. 45.
9. *Ma D.X., Xia Q.Y., Zhang C.* // J. At. Mol. Phys. – 2009. – **26**. – P. 361.
10. *Ma D.X., Xia Q.Y., Zhao W.W. et al.* // Comput. Appl. Chem. – 2009. – **26**. – P. 1583.
11. *McMurran J., Kouvetakis J., Nesting D.C. et al.* // J. Am. Chem. Soc. – 1998. – **120**. – P. 5233.
12. *Kouvetakis J., McMurran J., Steffek C. et al.* // Inorg. Chem. – 2000. – **39**. – P. 3805.
13. *Kouvetakis J., McMurran J., Steffek C. et al.* // Main Group Met. Chem. – 2001. – **24**. – P. 77.
14. *Becke A.D.* // J. Chem. Phys. – 1993. – **98**. – P. 5648.
15. *Lee C., Yang W., Parr R.G.* // Phys. Rev. B. – 1988. – **37**. – P. 785.
16. *Scott A.P., Radom L.* // J. Phys. Chem. – 1996. – **100**. – P. 16502.
17. *Frisch M.J., Trucks G.W., Schlegel H.B. et al.* Gaussian 03, Revision B.03. – Pittsburgh, PA, 2003.